Boosting Transport Distances for Molecular Excitons within Photo-excited Metal–Organic Framework Films

*Subhadip Goswami,[a] Michelle Chen,[a] Michael R. Wasielewski,[a] Omar K. Farha,[a,b] Joseph T. Hupp[a,c]**

[a]Department of Chemistry, Northwestern University, 2145 Sheridan Road, Evanston, IL 60208, United States
[b]Department of Chemistry, King Abdulaziz University, Jeddah 21589, Saudi Arabia
[c]Materials Science Division, Argonne National Laboratory, Argonne, Illinois 60439, United States

*To whom correspondence should be addressed.

ABSTRACT

Herein, we describe the fabrication of porphyrin-containing metal–organic framework (MOF) thin films with 1,4-diazabicyclo[2.2.2]octane (DABCO) pillaring linkers and investigate exciton transport within the films. Steady state emission spectroscopy indicates that the exciton can traverse up to 26 porphyrin layers when DABCO is used as a pillaring linker whereas on average only 9 to 11 layers can be traversed when either 4,4'-bipyridine (a pillaring linker) or pyridine (a non-pillaring, layer-interdigitating ligand) is used. These results can be understood by taking into account the decreased separation distances between transition-dipoles associated with chromophores (porphyrins) sited in adjacent layers. Shorter distances translate into faster Förster-type exciton hopping and, therefore, more hops within the few nanosecond lifetime of the porphyrin's singlet excited-state. The findings have favorable implications for the development of MOF-based photoelectrodes and photoelectrochemical energy-conversion devices.

Keywords: *metal−organic framework, layer-by-layer, energy transfer, transition dipole, exciton hopping*

INTRODUCTION

Visible-light-absorbing metal–organic frameworks (MOFs) constitute an increasingly attractive class of compounds for sensitization of solar-energy-conversion devices – both light-to-electrical and light-to-chemical energy conversion devices.[1-6] MOFs are porous (or potentially porous) two- or three-dimensional coordination polymers featuring organic linkers and inorganic nodes (single or multiple metal ions, or metal/non-metal clusters).[7-9] Typically they are crystalline, *i.e.* structurally well-defined. This property, together with the inherently modular nature of their assembly (from linkers and metal ions), has facilitated the experimental realization of an enormous variety of MOFs, and an even greater number *in silico.* Increasingly, new MOFs can be made to order.[10-15] Or, their likely structures, and resulting physical properties, can be predicted, given a set of synthesis conditions and chemical building blocks.[16-19]

Here we report on a light-absorbing 3D MOF featuring a well-studied architecture (the pillared paddlewheel),[20-21] redox-innocent nodes (pairs of zinc ions), an archetypal chromophore (free-base tetra(4-carboxylate-phenyl)-porphyrin (TCPP), and a nonchromophoric pillar (1,4-diazabicyclo[2.2.2]octane (DABCO)). With possible photoelectrochemical applications in mind, we constructed the MOF on glass or silicon surfaces using automated layer-by-layer (LbL) assembly, also termed liquid-phase epitaxy.[22-28] Our goal was to explore photo-initiated energy transfer and transport[29-32] – specifically, repetitive Förster-type energy transfer between consecutive pairs of chromophores residing in different, DABCO-separated, porphyrin layers, and ultimately, propagation of molecular excitons over extended distances. Among the attractions of LbL assembly are that it: a) permits control of MOF orientation relative to a solid support, b) offers the possibility of controlling MOF film thicknesses with close to single-molecule precision,[33] and c) allows for changes in the chemical identities of MOF building blocks over the course of film

growth, an effective way of creating well-defined redox gradients and/or energy transfer cascades.[34]

To employ MOF-based thin films in solar energy conversion devices, it is crucial that photogenerated excitons move through the framework with a high enough efficiency to reach a junction where they can productively dissociate into electrons and holes. For Förster-type energy transfer, exciton hopping rates are expected to increase strongly with decreasing separation distance between chromophores. For a process that is dominated by hopping along one dimension, the number of chromophore layers over which a molecular exciton can be propagated should scale as the square-root of the number of hops. Thus, for a given type of chromophore, shorter exciton hopping distances, r, should translate into more hops over the typically brief lifetime of the exciton, and propagation of the exciton over greater numbers of MOF molecular layers.

Previously, we explored the idea of boosting exciton migration by controllably collapsing a porphyrin-based MOF thin film from 3D pillared form to 2D-layered form.[35] Briefly, by replacing pillaring linkers (4,4'-bipyridine) with non-pillaring, layer-interdigitating, pyridine ligands, we found that the layer thickness (linker/ligand/node repeat-unit distance in the pillaring direction) could be compressed from about 15 Å to about 10 Å; see Scheme 1. Subsequent investigations of films spanning a range of pre-determined numbers of structural repeat layers, either without or with fluorescence quenchers at the film terminus, revealed that film compression engendered only a modest increase in efficacy of exciton propagation, *i.e.* from ~9 to 10 porphyrin layers to about 10 to 11 layers.[36] Thus, the improvement was considerably less than we had initially anticipated based on a limiting Förster-type $1/r^6$ scaling of exciton hopping rate. The explanation appears to lie in the distinction between layer spacing and transition-dipole/transition-dipole coupling distance (r). Film compression via replacement of ditopic 4,4'-bipyridine with monotopic pyridine

is accompanied by lateral displacement of porphyrin layers with respect to each other; see Scheme 1. If the porphyrins are approximated as point dipoles, film compression engenders almost no decrease in coupling distance, and, consequently, only marginal extension of exciton propagation.

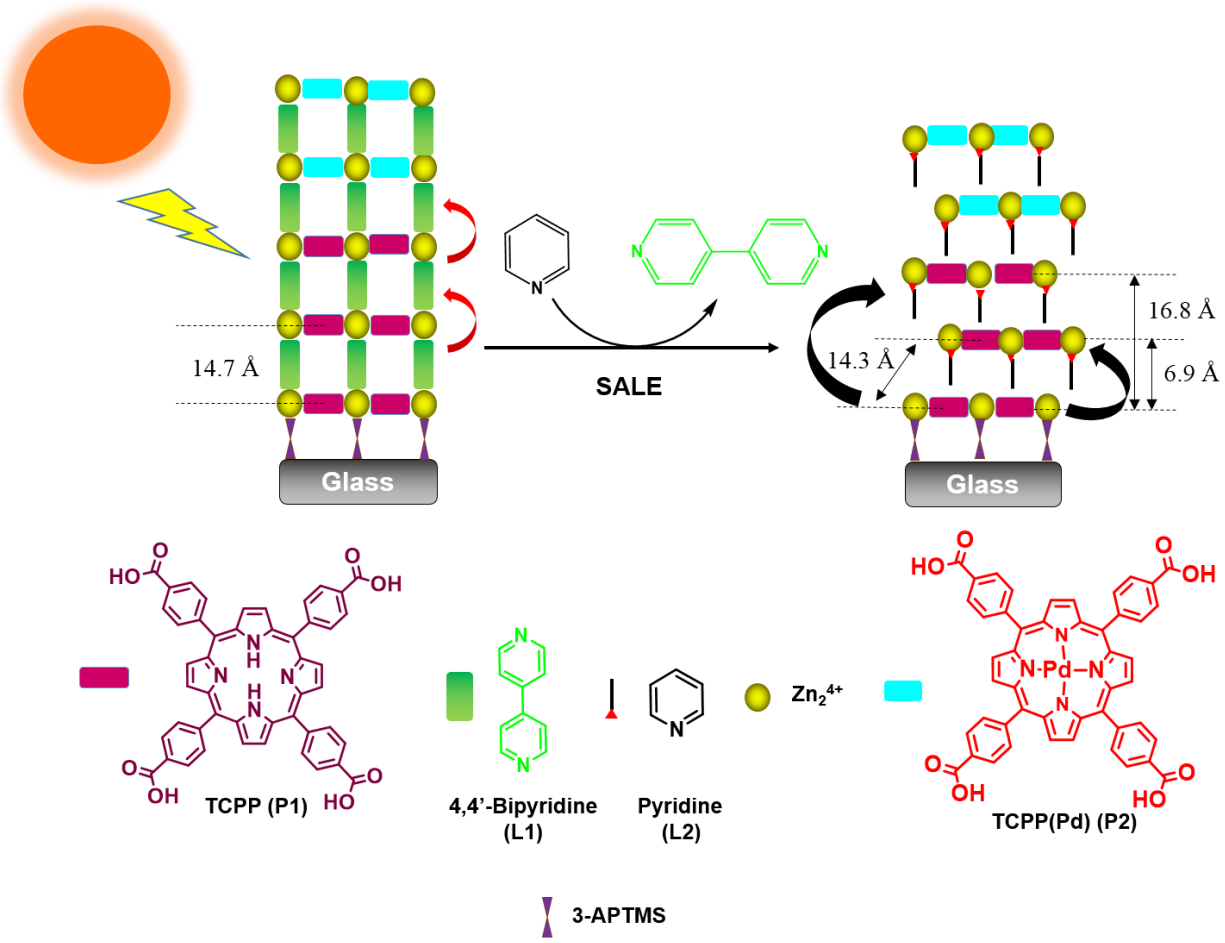

Scheme 1. Free base porphyrin TCPP (**P1)** and linker 4,4'-bipyridine (**L1)** were previously used to fabricate N (number of cycles) cycles of MOF thin films followed by N+1 and N+2 cycles by palladium porphyrin TCPP(Pd) (**P2)** and linker **L1**. SALE (Solvent assisted linker exchange) was performed with non-pillaring linker pyridine (**L2**) to replace **L1**. Vertical distances are inter-layer spacing (including layer thickness contributions to spacing). The indicated diagonal distance is the shortest inter-layer point-dipole to point-dipole distance between porphyrin **P1**. See ref. 35.

These findings suggest a revised strategy in which the spacing between porphyrin layers is decreased, but lateral displacement is absent. We reasoned that film assembly based on DABCO

pillars would extend the propagation of molecular excitons relative to both types of films in Scheme 1. Indeed, we find that the number of chromophoric layers through which photo-generated molecular excitons can be transmitted roughly triples.

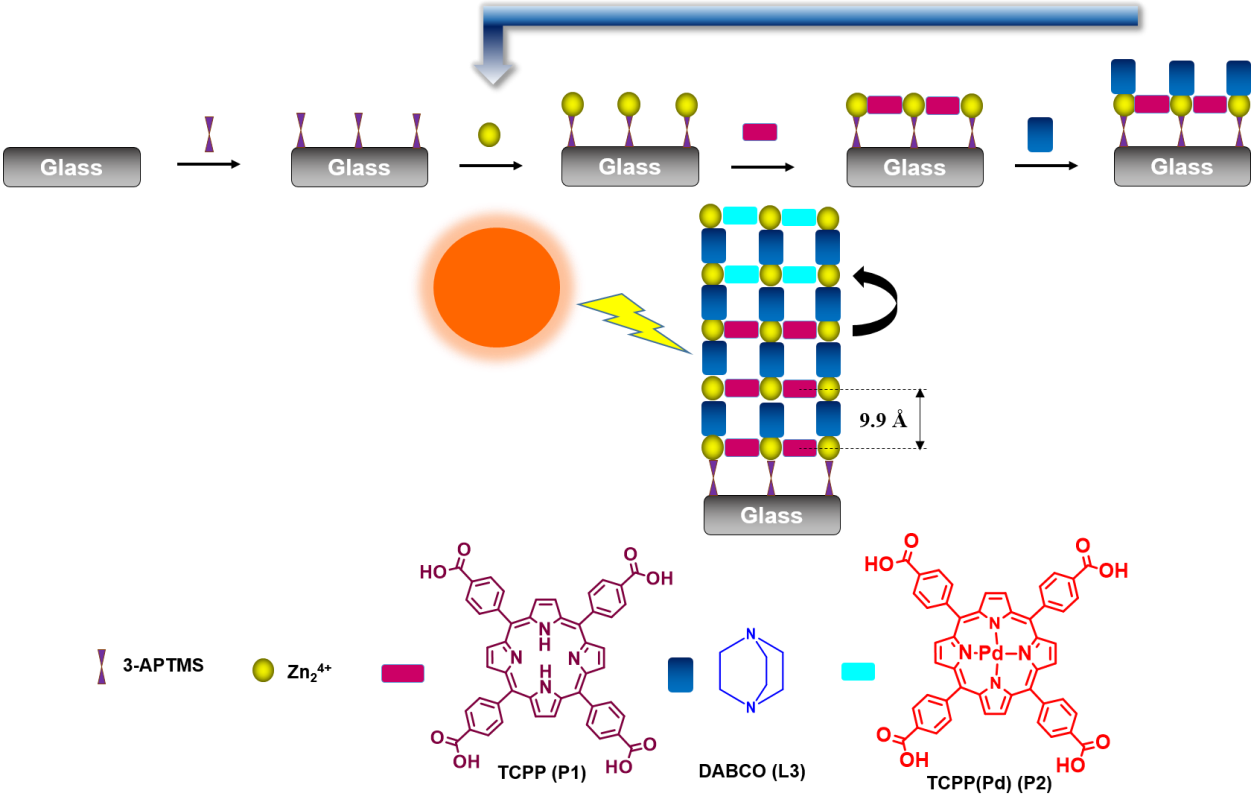

Scheme 2. Free-base porphyrin TCPP (**P1)** and linker **L3** were used to fabricate MOF thin films N growth cycles, followed by 2 cycles using a palladium-metallated porphyrin **P2** and linker **L3**. (**P1** and **P2** are incorporated as carboxylates rather than as carboxylic acids.) The vertical distance indicated is the shortest inter-layer point-dipole to point-dipole separation distance (see text).

EXPERIMENTAL

1. Materials

1,4-diazabicyclo[2.2.2]octane or DABCO, 4,4'-bipyridine, zinc acetate dihydrate and (3-aminopropyl) trimethoxysilane (3-APTMS) were purchased from Sigma-Aldrich and used without any further purification. Free base tetraphenylcarboxylate porphyrin **(H_4P1)** and ethanol were

obtained from Frontier Scientific and Fisher Scientific, respectively. The palladium porphyrin **(H_4P2)** used for the layer-by-layer synthesis was synthesized using a literature procedure.[37] Silicon wafers with a single sided resistance value of 20 KΩ/cm were obtained from University Wafers.

2. Fabrication of MOF thin films

Silicon wafers and glass substrates were pre-cleaned prior to the MOF film deposition by following a previously reported procedure.[33] First, the substrates were cut into 2.5 x 2.5 cm^2 pieces. Both type of substrates were cleaned by ultrasonication in a diluted Alconox solution, deionized water, isopropanol, and acetone sequentially for 20 min each. The substrates were further cleaned using a "Piranha solution" (3:1 v/v conc. H_2SO_4/30% H_2O_2) at room temperature for 1 h to further expose surface hydroxyl groups. **Safety Note:** *Piranha solution is highly corrosive. When working with piranha solution, care must be taken, and it is essential that proper PPE is worn (e.g. gloves, goggles, lab coat).* Deionized water was used to wash the substrates thoroughly and they were then dried in an oven at 90 °C for 30 min. Surface functionalization of the substrates were performed by soaking them in an 10 mM ethanolic solution of (3-aminopropyl) trimethoxysilane for 2 h followed by washing with copious amount of ethanol.

MOF thin films were deposited by using a computer controlled automated pump assembly as reported previously.[33] The substrates were soaked in a 0.1 mM zinc (II) acetate solution, 2 µM of **P1** and 20 µM DABCO (**L1**) in a sequential manner for 15 min each at 40 °C to deposit **"N"** cycles (N = number of LbL cycles). In between each step, the substrates were rinsed with pure ethanol twice for 7 minutes each to remove any unreacted substrates from the film. The final **"N+1"** and **"N+2"** cycles were exposed to 2 µM of **P2** while using the same concentration of zinc (II) acetate and DABCO solutions.

RESULTS AND DISCUSSION

Films were fabricated according to a previously described procedure using an automated pump assembly as outlined in Scheme 2.[33] In short, 3-aminopropyl-trimethoxysilane (3-APTMS) was used to functionalize the substrate which was then exposed sequentially to ethanolic solutions of 100 μM zinc(II)acetate, 2 μM **P1**, and 20 μM **L3** for 15 minutes each. For the final two LbL cycles, 2 μM **P2** was used in place of **P1** while the concentrations of Zn (II) precursor and **L3** were unchanged. Each of the exposure steps was followed by pump-driven rinsing with ethanol (twice) to remove physisorbed material. Based on previous reports by our group and others,[23, 33] we anticipated that one complete LbL cycle at these concentrations would add about one structural repeat unit ("one layer") of MOF material in the direction normal to the support. A series of **P1** films of varying thickness was constructed by using 13, 26, 39, or 52 LbL growth cycles.

Film thicknesses were estimated from profilometry measurements. For a 13-cycle film, the measured thickness was 10 ± 2 nm, implying a growth rate of ~0.8 nm/cycle.[38] In our experience with various measures of island-dominated LbL films, ellipsometry tends to yield values that match the tallest plateaus observed by profilometry, rather than an average of the plateaus and valleys evident in higher-resolution AFM measurements. The reported errors are those for these plateaus. From the published single-crystal X-ray structure of a closely related zinc-metallated porphyrin MOF (bulk sample) having DABCO as the pillaring ligand,[39] the layer thickness is ~ 0.99 nm. Thus, each LbL cycle adds, on average, about 0.8 MOF layers. For 26, 39, and 52 LbL cycles, the measured thicknesses were 16, 26, and 42 nm, respectively. It should be noted that the film growth rate for the 26 and 39 cycle films is slower than that of 13 cycle films, consistent with previous reports where, due to island formation, faster growth was observed in the early stages of film formation.[40-41]

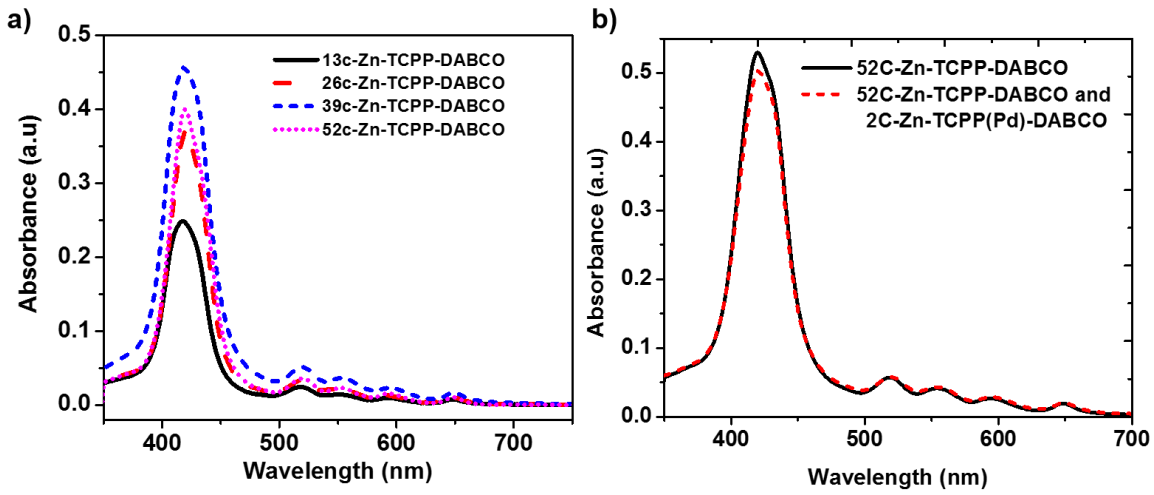

Figure 1. a) Electronic absorption spectra of 13C, 26C, 39C, and 52C LbL films (black solid, red dashed, blue short dash and pink dot traces), grown on transparent glass substrates, b) electronic absorption spectra of 39C-Zn-TCPP-DABCO before (solid black) and after (red dashed) the addition of 2C-TCPP(Pd). (The notation Zn-TCPP-DABCO refers to films based on pairs of Zn(II) ions as node, free-base porphyrin TCPP units as tetracarboxylated linkers and DABCO molecules as pillaring linkers. TCPP(Pd) denotes TCCP with Pd(II) coordinated by the pyrrolic nitrogens.)

Figure 1a shows absorption spectra for four films (13, 26, 39, and 52 cycles) grown on 3-APTMS functionalized glass supports. The spectra feature an intense Soret band at ~ 420 nm and four Q-bands (518, 556, 594 and 648 nm). The observation of four Q-bands indicates that the free-base porphyrin units resist metalation, despite repetitive exposure to zinc(II) during film fabrication. The resistance to metalation is presumably a consequence of both the very low Zn(II) concentration (relative to typical bulk MOF syntheses, where metal ion recruitment by porphyrins occurs spontaneously) and the comparatively low assembly temperature (40^{o}C versus 80^{o}C or higher for typical bulk syntheses). Gradual increases in film electronic absorption are obtained as the number of LbL growth cycles increases.

Shown in Figure 1b are absorption spectra for a 52 cycle film of Zn-TCPP-DABCO before and after two additional growth cycles using TCPP(Pd) (**P2**) in place of **P1**. Notably, the spectra are only marginally different. Similar results were obtained with other films.

The average orientation of the porphyrin molecules within the MOF thin films was probed via polarized absorption spectroscopy and an example is shown for a 39 cycle film in Figure S1. In accordance with previous reports,[33, 35] the porphyrins are found to be oriented parallel to the glass support – the optimal orientation for light absorption from a source positioned normal to the film.

Following our previous report,[35] exciton transport was investigated by evaluating quenching of MOF film fluorescence by an energy acceptor (TCPP(Pd), **P2**) sited at the outer edge of the film. Figure 2 shows emission profiles of N Cycle-LbL and (N + 2C) Cycle LbL MOF films, where N is the number of LbL cycles **P1** (13, 26, 39, or 52) and "+ 2C" denotes 2 cycles of **P2**. All films were excited at 420 nm, and emission was monitored from 625 to 800 nm. In all cases, emission characteristic of the fluorescence of the free-base porphyrin was observed. When TCPP(Pd) is installed, significant emission quenching is observed for DABCO-pillared films of all thicknesses. For the 13C, 26C, and 39C films, **P2** quenches the emission of **P1** by more than 50%. Given the sharp fall-off of energy transfer rates with transition-dipole/transition-dipole separation distance, significant direct energy transfer from photo-excited **P1** units to **P2** should be possible only for **P1** units located directly next to **P2**, or perhaps one layer removed. Thus, for a 10-layer film (13 LbL growth cycles), direct energy transfer from photo-excited free-base porphyrins to TCCP(Pd) should engender at most only 10 to 20% quenching. The balance of the quenching can be attributed to transport of remotely generated molecular excitons, via **P1**→**P1** exciton hopping, to sites proximal to the quencher, **P2**, at the terminus of the film.

Time resolved fluorescence (TRF) experiments were performed for a representative set of compositions: 13C-Zn-TCPP-DABCO films, with and without terminal TCPP(Pd) layers. Samples were excited at 420 nm and fluorescence decays were fit at 660 nm (Figure S4). For 13C-Zn-TCPP-DABCO, a faster component and a slower component were observed with lifetimes of 70 ± 27 ps and 9.1 ± 2.3 ns, respectively.[42] After the incorporation of quencher, the slower component was not observed, but a fast component with a time constant of 73 ± 27 ps persisted. The identical time constants for the fast component, without and with TCPP(Pd) quenching layers, implies that the chromophore sub-population responsible for the short component is immune to quenching and that the residual fluorescence observed in the corresponding steady-state experiments is due to this sub-population. It is tempting to speculate that the fast component is associated with a MOF structural defect such as a TCPP aggregate. With this in mind, we measured emission spectra for the short- and long-lived components (Figure S6); the data are noisy, but no clear difference is evident.

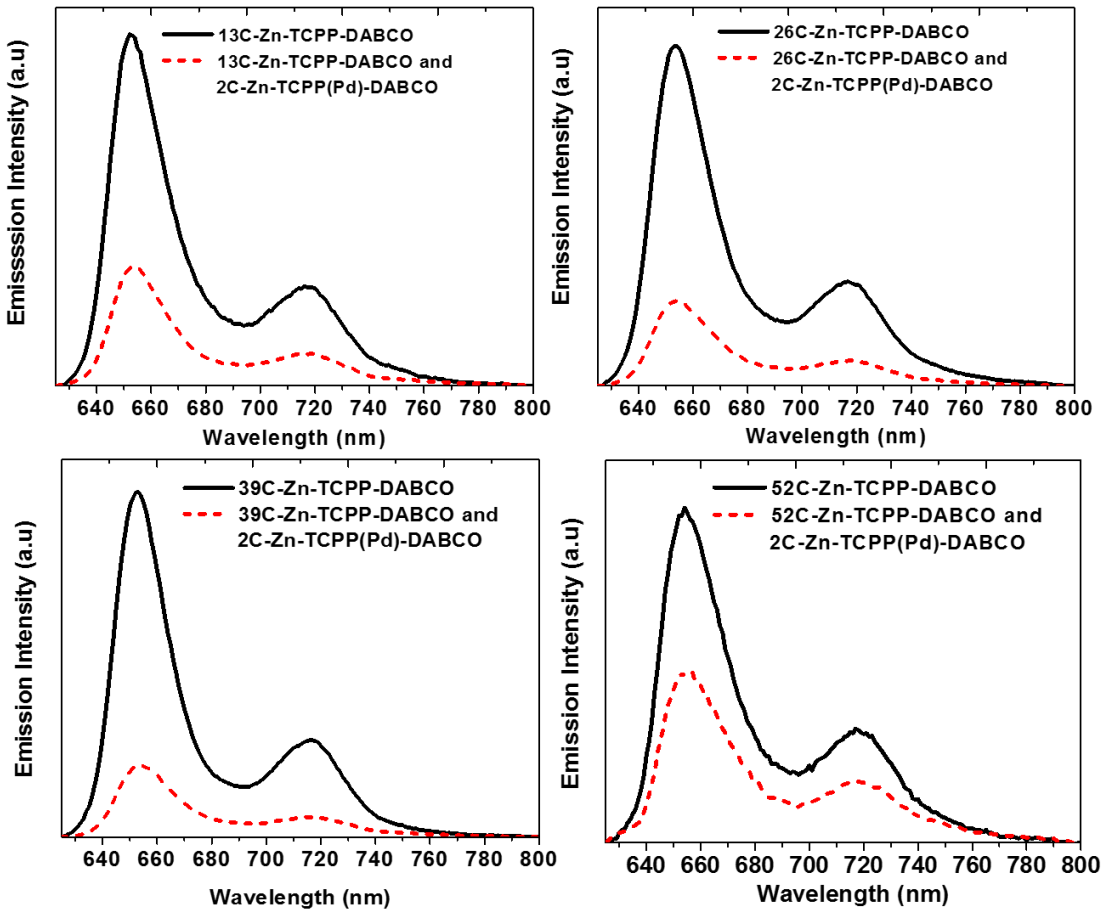

Figure 2. Steady-state emission spectra of N cycle-LbL and (N + 2) cycle LbL films (where, N = 13, 26, 39 and 52) measured on glass substrates. The N cycle LbL spectra are shown with black solid lines and (N + 2) cycle LbL spectra are shown with red dashed lines. In each case, the N and (N + 2) pair corresponding to the same **P1** film, *i.e.* spectra were recorded before and after **P2** LbL addition to a given film initially with **P1** All films were excited at 420 nm.

Figure 3a contains a plot of the extent of film quenching by **P2** as a function of the number of **P1** layers in each DABCO-pillared film. Also plotted are previous results for films featuring either 4,4'-bipyridine or pyridine in place of DABCO (together with new data collected for films either 7 or 12 layers thick). Notably, extrapolation of the plots to the limit of a single **P1** layer does not culminate in 100% quenching. From the above-mentioned lifetime experiments it is clear that the residual steady-state fluorescence emission is associated with the short-lived component.

Evidently the excitons associated with this component, in contrast to their much longer-lived counterparts, are incapable of moving through even a small number of layers and reaching the **P2**-based quenching layers.

In our previous study we (incorrectly) assumed that all excitons are equally mobile, both because of common lifetimes and common hopping rates. Thus, we assumed that all excitons formed within a few to several layers of the film terminus can reach the terminus and be quenched by **P2**. The time-resolved luminescence measurements, showing selective quenching of long-lived excitons, belie these assumptions. In our earlier report, by mistakenly assuming similar transport efficacy for all excitons, we slightly underestimated for both pyridine and 4,4'-bipyridine films the number of **P1** layers over which *long-lived* excitons can propagate. Figure 3b takes into account this difference. The y-axis is now labeled "percent quenched, after correction for residual emission," and the data are again plotted versus the number of MOF layers in the film. The product of the corrected emission and the number of **P1** layers illuminated (*i.e.*, present) yields the maximum number of layers (on average) over which the long-lived exciton can be propagated. Thus, free-base porphyrin MOF films containing 4,4'-bipyridine pillars or interdigitating pyridine ligands can effectively transport long-lived excitons through a maximum of *ca.* 9-10 or 10-11 layers, respectively; see Table 1. (See Section S3 of the Supplemental Information for details.[43])

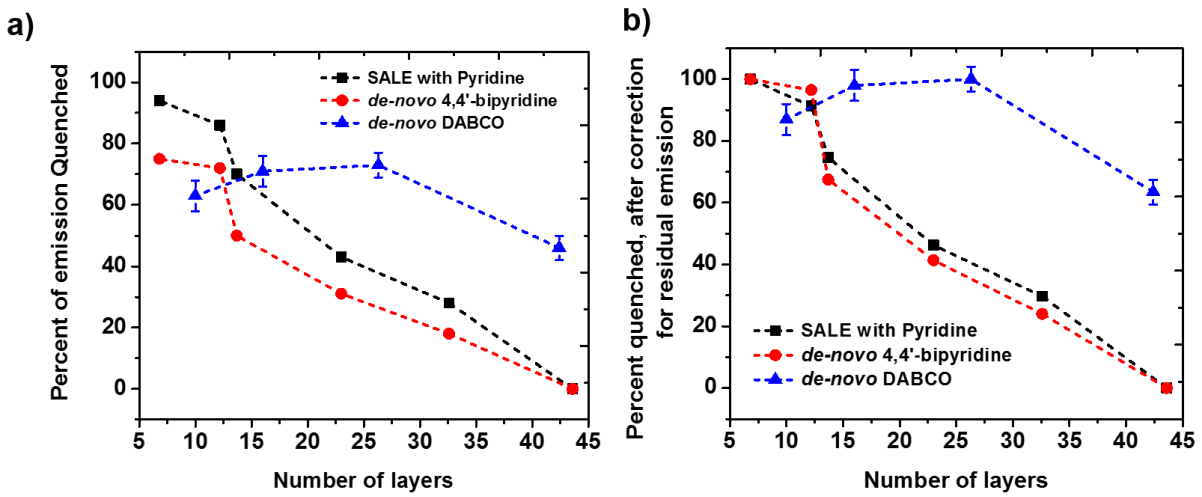

Figure 3. a) Plots of percent of emission quenched for (N-C +2C)-LbL MOF films as a function of the number of layers of emissive **P1** present, with DABCO (blue triangles), pyridine (black squares), or 4,4'-bipyridine (red circles) as pillaring or interdigitating ligands. b) Data replotted to correct for residual emission from inefficient quenching of a subpopulation of excitons characterized by a short lifetime. For *de novo* DABCO-pillared films, each of the plotted values for percent of emission quenched is an average of measurements for three independently fabricated films. Values plotted for *de novo* 4,4'-bipyridine-pillared films and for SALE-derived, pyridine-containing films assembled via 13, 26, 39, or 52 **P1** growth cycles, were derived from previously published measurements as described in the text. Values shown for 4,4'-bipyridine- or pyridine-containing films assembled via 5 or 8 **P1** growth cycles are each averages for two independently fabricated films.

From Figure 3b, and Table 2, excitons in suitably thick DABCO-pillared films can traverse about three times as many (**P1**) MOF layers (~26) as those in 4,4'-bipyridine-pillared films (~9-10). (Obviously, the distance over which excitons can be propagated cannot exceed the physical thickness of the film.) A curious finding, evident in both Table 1 and Table 2, is that for films exceeding a critical thickness, excitons travel slightly less far than for films not exceeding this thickness. Thus, for the thickest DABCO-pillared films (*ca.* 42 **P1** layers), excitons are propagated through ~22 **P1** layers rather than ~26.[44] The difference presumably reflects the fact that for thinner films, exciton transport away from the quenching layer is significantly bounded by the thickness of the film itself, while for thicker films, excitons are less constrained and can sample layers that

are further from the quenching layer. While perhaps obvious in retrospect, the finding has implications for the design of light-absorbing, MOF films for energy-conversion applications.[45]

Table 1. Revised estimates of the maximum number of layers the exciton traverses in **P1**-based MOF films featuring either 4,4'-bipyridine pillars[46] or interdigitating pyridine ligands. Estimates derived from steady-state fluorescence quenching experiments.

Number of P1 film growth cycles	Number of P1 layers deposited [a]	Number of P1 layers traversed with 4,4'-bipyridine pillars	Number of P1 layers traversed with pyridine ligands
5	7	7	7
8	12	12	11
13	14	9	10
26	23	9	10
39	33	8	10
52	44	–[b]	–[b]

a. Each value is an average from measurements of three independently prepared films corresponding to three independent LbL MOF fabrication super-cycles.

b. Quenching not detected.

Table 2. The maximum number of layers the exciton traverses with DABCO as pillaring ligand, derived from steady state fluorescence quenching experiments.

Number of film P1 growth cycles	Number of P1 layers deposited	Number of P1 layers traversed with DABCO pillars
13	10	9
26	16	16
39	26	26
52	42	22

Layer-to-layer exciton hopping distances are ~10 and 14.7 Å, respectively, for DABCO- and 4,4,-bipyridine-pillared porphyrin films. In the point-dipole limit for describing porphyrin

chromophores, these distances can be identified with the quantity r in Förster theory – which promises that exciton hopping rates will vary as $1/r^6$. Thus, the ratio of layer-to-layer (**P1 → P1**) energy transfer rates for DABCO vs. 4,4'-bipyridine films should be $(1.47)^6$, *i.e.* ~10. If hopping within layers is much slower than hopping between layers, excitons will move mainly in directions normal to the glass support. In the absence of an energy gradient, exciton transport should be diffusive and the number of inter-layer spacings across which the exciton can be moved (*i.e.*, one less than the number of layers traversed) should scale as the square-root of the number of hops that can be executed within the lifetime of the porphyrin singlet excited-state. Thus, for DABCO vs. 4,4'-bipyridine films the anticipated ratio of exciton displacement (in terms of porphyrin-porphyrin layer spacings) is $(1.47)^3$, *i.e.* ~3.2.

The observed ratio of ~22-26 (DABCO) to ~8-9 (4,4'-bipyridine) compares well with the Förster prediction. From the agreement, we infer that: a) the point-dipole model is satisfactory for the hopping distances examined, and b) the assumption that energy transport is significant only between porphyrin layers, and not within layers, is likely correct. Thus, the largely one-dimensional energy transport through these types of MOFs (2D sheets of planar chromophores separated by pillars) presents an interesting contrast to transport within various Ru(2,2'-bipyridine)$_3$-derived MOFs for which energy transfer is equally probable (or nearly so) in the x, y, and z directions, *i.e.* isotropically three-dimensional. (A further difference is the reliance upon Dexter-type transfer, at least in some instances – for example, to propagate excitons through Ru(2,2'-bipyridine)$_3$-type films.)[47-49]

As points of reference, it is worth comparing the LbL porous film results with findings based on other modes of film tetra-phenyl porphyrin (TPP) formation (albeit, films of little or no significant porosity). Polomaki, *et al.* used repetitive, copper-catalyzed, alkyne/azide click

chemistry to grow porphyrin multilayers on conductive-glass electrodes. From photoelectrochemical measurements, exciton transport appears to range from 3 to 5 porphyrin layers.[50] Huijser, *et al.*[51] and subsequently Kaushal, *et al.*,[30] showed that with appropriate peripheral chemical derivatization, exciton transport within solvent-deposited films of TPP and Zn-TPP, respectively, could be boosted from just a few molecular layers to as many as ~14 layers. The beneficial role of substituents is to organize chromophores into layers resembling classic self-assembled alkane-thiol monolayers or related structures.

CONCLUSIONS

We find that transport distances for photo-generated molecular excitons in porphyrin-based LbL-grown MOF films can be usefully extended (roughly tripled) by replacing bipyridine pillars with shorter pillars (DABCO), provided that attention is paid to the distinction between chromophoric layer separation distances and essentially point-dipole/point-dipole distances. An approximate tripling of the transport distance is expected (from simple Förster theory) if exciton transport is primarily one-dimensional, with much smaller enhancements if transport is effectively two- or three-dimensional. Thus, the observations here are consistent with an LbL MOF-film architecture that constrains energy-transfer and -transport primarily to forward or reverse directions normal to the underlying support (*i.e.* between 2D-porphyrin layers, rather than laterally within a layer). With anisotropic energy transport over sizable distances now demonstrated, our efforts going forward are focused, in part, on extending transport yet further, with the aim of productively capturing more light. In principle, shorter pillars could be used, although it is difficult to envision what those pillars might be. Alternatively, if the tetra-phenyl-porphyrin chromophore were replaced with a porphyrin of significantly lower symmetry, the nominally forbidden Q-band absorptions would become strongly allowed,[52-56] resulting in much stronger overlap between

absorption and emission spectra and much faster Förster energy transfer. (The symmetry reduction also would serve to enhance spectral coverage by boosting red absorption.) If the faster transfer were accompanied by comparatively little change in singlet-excited-state lifetime, faster energy transfer would result in exciton transport through greater numbers of MOF chromophoric layers and greater physical distances. A second attractive approach to extending transport distances would be to build-in an energy gradient (via use of multiple, overlapping chromophores), as this would bias excitons toward transport in one direction, *i.e.* toward lower energy.[34] We hope to address both issues experimentally in the not-too-distant future. We also hope to address soon the issue of productively splitting transported excitons to drive redox catalysts and/or convert solar energy to electrical energy.

ASSOCIATED CONTENT

Supporting Information. Specifics on materials used, fabrication of MOF thin films, instrumentation, and MOF film structural characterization are available here. This material is available free of charge via the Internet at http://pubs.acs.org.

AUTHOR INFORMATION

Corresponding Author

* E-mail: j-hupp@northwestern.edu

ORCID

Subhadip Goswami **0000-0002-8462-9054**
Michelle Chen **0000-0002-4336-2971**
Michael R. Wasielewski **0000-0003-2920-5440**
Omar K. Farha **0000-0002-9904-9845**
Joseph T. Hupp **0000-0003-3982-9812**

ACKNOWLEDGMENTS

We gratefully acknowledge support from the U.S. Dept. of Energy, Office of Science, Office of Basic Energy Sciences (grant no. DE-FG02-87ER13808 (SG, J.T.H and O.K.F), grant no. DE-FG02- 99ER14999 (M.C and M.R.W)) and Northwestern University. We also thank Dr. Alex Martinson (Argonne National Laboratory) for advice and help with polarized absorption measurements.

References

1. Lee, C. Y.; Farha, O. K.; Hong, B. J.; Sarjeant, A. A.; Nguyen, S. T.; Hupp, J. T., Light-Harvesting Metal–Organic Frameworks (MOFs): Efficient Strut-to-Strut Energy Transfer in Bodipy and Porphyrin-Based MOFs. *J. Am. Chem. Soc.* **2011,** *133*, 15858-15861.
2. Son, H.-J.; Jin, S.; Patwardhan, S.; Wezenberg, S. J.; Jeong, N. C.; So, M.; Wilmer, C. E.; Sarjeant, A. A.; Schatz, G. C.; Snurr, R. Q.; Farha, O. K.; Wiederrecht, G. P.; Hupp, J. T., Light-Harvesting and Ultrafast Energy Migration in Porphyrin-Based Metal–Organic Frameworks. *J. Am. Chem. Soc.* **2013,** *135*, 862-869.
3. Kent, C. A.; Liu, D.; Ma, L.; Papanikolas, J. M.; Meyer, T. J.; Lin, W., Light Harvesting in Microscale Metal–Organic Frameworks by Energy Migration and Interfacial Electron Transfer Quenching. *J. Am. Chem. Soc.* **2011,** *133*, 12940-12943.
4. Liu, J.; Zhou, W.; Liu, J.; Howard, I.; Kilibarda, G.; Schlabach, S.; Coupry, D.; Addicoat, M.; Yoneda, S.; Tsutsui, Y.; Sakurai, T.; Seki, S.; Wang, Z.; Lindemann, P.; Redel, E.; Heine, T.; Wöll, C., Photoinduced Charge-Carrier Generation in Epitaxial MOF Thin Films: High Efficiency as a Result of an Indirect Electronic Band Gap? *Angew. Chem. Int. Ed.* **2015,** *54*, 7441-7445.
5. Spoerke, E. D.; Small, L. J.; Foster, M. E.; Wheeler, J.; Ullman, A. M.; Stavila, V.; Rodriguez, M.; Allendorf, M. D., MOF-Sensitized Solar Cells Enabled by a Pillared Porphyrin Framework. *J. Phys. Chem. C* **2017,** *121*, 4816-4824.
6. Maza, W. A.; Haring, A. J.; Ahrenholtz, S. R.; Epley, C. C.; Lin, S. Y.; Morris, A. J., Ruthenium(II)-Polypyridyl Zirconium(IV) Metal-Organic Frameworks as a New Class of Sensitized Solar Cells. *Chem.Sci.* **2016,** *7*, 719-727.
7. Rowsell, J. L. C.; Yaghi, O. M., Metal–Organic Frameworks: A New Class of Porous Materials. *Microporous Mesoporous Mater.* **2004,** *73*, 3-14.
8. Zhou, H.-C.; Long, J. R.; Yaghi, O. M., Introduction to Metal–Organic Frameworks. *Chem. Rev.* **2012,** *112*, 673-674.
9. Batten, S. R.; Champness, N. R.; Chen, X.-M.; Garcia-Martinez, J.; Kitagawa, S.; Ohrstrom, L.; O'Keeffe, M.; Suh, M. P.; Reedijk, J., Coordination Polymers, Metal-Organic Frameworks and the Need for Terminology Guidelines. *CrystEngComm* **2012,** *14*, 3001-3004.
10. Li, P.; Vermeulen, N. A.; Malliakas, C. D.; Gómez-Gualdrón, D. A.; Howarth, A. J.; Mehdi, B. L.; Dohnalkova, A.; Browning, N. D.; O'Keeffe, M.; Farha, O. K., Bottom-up Construction of a Superstructure in a Porous Uranium-Organic Crystal. *Science* **2017,** *356*, 624-627.
11. Chen, Z.; Weseliński, Ł. J.; Adil, K.; Belmabkhout, Y.; Shkurenko, A.; Jiang, H.; Bhatt, P. M.; Guillerm, V.; Dauzon, E.; Xue, D.-X.; O'Keeffe, M.; Eddaoudi, M., Applying the Power of Reticular Chemistry to Finding the Missing Alb-Mof Platform Based on the (6,12)-Coordinated Edge-Transitive Net. *J. Am. Chem. Soc.* **2017,** *139*, 3265-3274.
12. Alezi, D.; Peedikakkal, A. M. P.; Weseliński, Ł. J.; Guillerm, V.; Belmabkhout, Y.; Cairns, A. J.; Chen, Z.; Wojtas, Ł.; Eddaoudi, M., Quest for Highly Connected Metal–Organic Framework Platforms: Rare-Earth Polynuclear Clusters Versatility Meets Net Topology Needs. *J. Am. Chem. Soc.* **2015,** *137*, 5421-5430.
13. Catarineu, N. R.; Schoedel, A.; Urban, P.; Morla, M. B.; Trickett, C. A.; Yaghi, O. M., Two Principles of Reticular Chemistry Uncovered in a Metal–Organic Framework of

Heterotritopic Linkers and Infinite Secondary Building Units. *J. Am. Chem. Soc.* **2016,** *138*, 10826-10829.
14. O'Keeffe, M.; Yaghi, O. M., Deconstructing the Crystal Structures of Metal–Organic Frameworks and Related Materials into Their Underlying Nets. *Chem. Rev.* **2012,** *112*, 675-702.
15. Alezi, D.; Spanopoulos, I.; Tsangarakis, C.; Shkurenko, A.; Adil, K.; Belmabkhout, Y.; O′Keeffe, M.; Eddaoudi, M.; Trikalitis, P. N., Reticular Chemistry at Its Best: Directed Assembly of Hexagonal Building Units into the Awaited Metal-Organic Framework with the Intricate Polybenzene Topology, Pbz-MOF. *J. Am. Chem. Soc.* **2016,** *138*, 12767-12770.
16. Chung, Y. G.; Gómez-Gualdrón, D. A.; Li, P.; Leperi, K. T.; Deria, P.; Zhang, H.; Vermeulen, N. A.; Stoddart, J. F.; You, F.; Hupp, J. T.; Farha, O. K.; Snurr, R. Q., In Silico Discovery of Metal-Organic Frameworks for Precombustion CO2 Capture Using a Genetic Algorithm. *Science Advances* **2016,** *2*, e1600909.
17. Witman, M.; Ling, S.; Anderson, S.; Tong, L.; Stylianou, K. C.; Slater, B.; Smit, B.; Haranczyk, M., In Silico Design and Screening of Hypothetical MOF-74 Analogs and Their Experimental Synthesis. *Chem.Sci.* **2016,** *7*, 6263-6272.
18. Zhang, C.; Han, C.; Sholl, D. S.; Schmidt, J. R., Computational Characterization of Defects in Metal–Organic Frameworks: Spontaneous and Water-Induced Point Defects in ZIF-8. *J. Phys. Chem. Lett.* **2016,** *7*, 459-464.
19. Martin, R. L.; Lin, L.-C.; Jariwala, K.; Smit, B.; Haranczyk, M., Mail-Order Metal–Organic Frameworks (MOFs): Designing Isoreticular Mof-5 Analogues Comprising Commercially Available Organic Molecules. *J. Phys. Chem. C* **2013,** *117*, 12159-12167.
20. Burnett, B. J.; Barron, P. M.; Hu, C.; Choe, W., Stepwise Synthesis of Metal–Organic Frameworks: Replacement of Structural Organic Linkers. *J. Am. Chem. Soc.* **2011,** *133*, 9984-9987.
21. Islamoglu, T.; Goswami, S.; Li, Z.; Howarth, A. J.; Farha, O. K.; Hupp, J. T., Postsynthetic Tuning of Metal–Organic Frameworks for Targeted Applications. *Acc. Chem. Res.* **2017,** *50*, 805-813.
22. Zacher, D.; Shekhah, O.; Woll, C.; Fischer, R. A., Thin Films of Metal-Organic Frameworks. *Chem. Soc. Rev.* **2009,** *38*, 1418-1429.
23. Zacher, D.; Yusenko, K.; Bétard, A.; Henke, S.; Molon, M.; Ladnorg, T.; Shekhah, O.; Schüpbach, B.; de los Arcos, T.; Krasnopolski, M.; Meilikhov, M.; Winter, J.; Terfort, A.; Wöll, C.; Fischer, R. A., Liquid-Phase Epitaxy of Multicomponent Layer-Based Porous Coordination Polymer Thin Films of [M(L)(P)0.5] Type: Importance of Deposition Sequence on the Oriented Growth. *Chem. Eur. J.* **2011,** *17*, 1448-1455.
24. Shekhah, O., Layer-by-Layer Method for the Synthesis and Growth of Surface Mounted Metal-Organic Frameworks (Surmofs). *Materials* **2010,** *3*, 1302.
25. Shekhah, O.; Wang, H.; Kowarik, S.; Schreiber, F.; Paulus, M.; Tolan, M.; Sternemann, C.; Evers, F.; Zacher, D.; Fischer, R. A.; Wöll, C., Step-by-Step Route for the Synthesis of Metal−Organic Frameworks. *J. Am. Chem. Soc.* **2007,** *129*, 15118-15119.
26. Chernikova, V.; Shekhah, O.; Spanopoulos, I.; Trikalitis, P. N.; Eddaoudi, M., Liquid Phase Epitaxial Growth of Heterostructured Hierarchical Mof Thin Films. *Chem. Commun.* **2017,** *53*, 6191-6194.
27. Shekhah, O.; Fu, L.; Sougrat, R.; Belmabkhout, Y.; Cairns, A. J.; Giannelis, E. P.; Eddaoudi, M., Successful Implementation of the Stepwise Layer-by-Layer Growth of MOF Thin Films on Confined Surfaces: Mesoporous Silica Foam as a First Case Study. *Chem. Commun.* **2012,** *48*, 11434-11436.

28. Stavila, V.; Schneider, C.; Mowry, C.; Zeitler, T. R.; Greathouse, J. A.; Robinson, A. L.; Denning, J. M.; Volponi, J.; Leong, K.; Quan, W.; Tu, M.; Fischer, R. A.; Allendorf, M. D., Thin Film Growth of Nbo MOFs and Their Integration with Electroacoustic Devices. *Adv. Funct. Mater.* **2016,** *26*, 1699-1707.
29. Dolgopolova, E. A.; Williams, D. E.; Greytak, A. B.; Rice, A. M.; Smith, M. D.; Krause, J. A.; Shustova, N. B., A Bio-Inspired Approach for Chromophore Communication: Ligand-to-Ligand and Host-to-Guest Energy Transfer in Hybrid Crystalline Scaffolds. *Angew. Chem. Int. Ed.* **2015,** *54*, 13639-13643.
30. Kaushal, M.; Ortiz, A. L.; Kassel, J. A.; Hall, N.; Lee, T. D.; Singh, G.; Walter, M. G., Enhancing Exciton Diffusion in Porphyrin Thin Films Using Peripheral Carboalkoxy Groups to Influence Molecular Assembly. *J. Mater. Chem. C*, **2016,** *4*, 5602-5609.
31. Huijser, A.; Savenije, T. J.; Kroeze, J. E.; Siebbeles, L. D. A., Exciton Diffusion and Interfacial Charge Separation in Meso-Tetraphenylporphyrin/TiO_2 Bilayers: Effect of Ethyl Substituents. *J. Phys. Chem. B* **2005,** *109*, 20166-20173.
32. Kroeze, J. E.; Savenije, T. J.; Warman, J. M., Efficient Charge Separation in a Smooth-TiO2/Palladium-Porphyrin Bilayer Via Long-Distance Triplet-State Diffusion. *Adv. Mater.* **2002,** *14*, 1760-1763.
33. So, M. C.; Jin, S.; Son, H.-J.; Wiederrecht, G. P.; Farha, O. K.; Hupp, J. T., Layer-by-Layer Fabrication of Oriented Porous Thin Films Based on Porphyrin-Containing Metal–Organic Frameworks. *J. Am. Chem. Soc.* **2013,** *135*, 15698-15701.
34. Park, H. J.; So, M. C.; Gosztola, D.; Wiederrecht, G. P.; Emery, J. D.; Martinson, A. B. F.; Er, S.; Wilmer, C. E.; Vermeulen, N. A.; Aspuru-Guzik, A.; Stoddart, J. F.; Farha, O. K.; Hupp, J. T., Layer-by-Layer Assembled Films of Perylene Diimide- and Squaraine-Containing Metal–Organic Framework-Like Materials: Solar Energy Capture and Directional Energy Transfer. *ACS Appl. Mater. Interfaces* **2016,** *8*, 24983-24988.
35. Goswami, S.; Ma, L.; Martinson, A. B. F.; Wasielewski, M. R.; Farha, O. K.; Hupp, J. T., Toward Metal–Organic Framework-Based Solar Cells: Enhancing Directional Exciton Transport by Collapsing Three-Dimensional Film Structures. *ACS Appl. Mater. Interfaces* **2016,** *8*, 30863-30870.
36. These numbers are slightly greater than what we reported previously because we are no longer assuming (incorrectly) that all nearby excitons, including short-lived excitons, are quantitatively quenchable by Pd-porphyrins (see text for details).
37. Farha, O. K.; Shultz, A. M.; Sarjeant, A. A.; Nguyen, S. T.; Hupp, J. T., Active-Site-Accessible, Porphyrinic Metal−Organic Framework Materials. *J. Am. Chem. Soc.* **2011,** *133*, 5652-5655.
38. Atomic force microscopy (AFM) measurements, which are inherently higher in spatial resolution than profilometry, show films to be considerably rougher (Figure S2 in Supplemental Information) than indicated by profilometry. In our discussion of exciton transport distances we neglect film roughness. Thus, the reported distances likely correspond to lower-limit estimates of the true transport distances. Work in progress is aimed at identifying and largely eliminating the chemical factors responsible for LbL MOF film roughness.
39. Sakuma, T.; Sakai, H.; Araki, Y.; Wada, T.; Hasobe, T., Control of Local Structures and Photophysical Properties of Zinc Porphyrin-Based Supramolecular Assemblies Structurally Organized by Regioselective Ligand Coordination. *PCCP* **2016,** *18*, 5453-5463.

40. Ohnsorg, M. L.; Beaudoin, C. K.; Anderson, M. E., Fundamentals of MOF Thin Film Growth Via Liquid-Phase Epitaxy: Investigating the Initiation of Deposition and the Influence of Temperature. *Langmuir* **2015,** *31,* 6114-6121.
41. Summerfield, A.; Cebula, I.; Schröder, M.; Beton, P. H., Nucleation and Early Stages of Layer-by-Layer Growth of Metal Organic Frameworks on Surfaces. *J. Phys. Chem. C* **2015,** *119*, 23544-23551.
42. In our previous report, measurements extended to only 1 ns – too short to reveal the presence of a low-amplitude 9 ns decay component(Ref.35).
43. At the same time, as noted above, a sub-population of short-lived excitons displays a resistance to fluorescence quenching that appears insensitive to MOF film thickness, at least over the range of thicknesses probed. It is tempting to equate the relative intensities of P2-quenchable and non-quenchable emission with the population ratio of long-lived excitons to short-lived excitons, and thereby gain insight into the density of putative aggregate or defect sites. Unfortunately, we lack needed information about emission quantum yields for long- vs. short-lived excitons, as well as information about the number of chromophores over which short-lived excitons may be delocalized.
44. For quenching measurements, illumination is done from the Pd-porphyrin side of the film and we assume that fluorescence is dominated by free-base porphyrins sited furthest from the Pd-porphyrin quenching layers. These constitute about 38% of the photo-excited porphyrins. The Soret-peak absorbance for a 54-cycle film is ~0.5, and corresponds to absorption of ~68% of the incident photons, i.e. 100% x (1 - 10-Abs) = 100% x (1 - 10-0.5). To remove 62% of the absorbed photons, an absorbance of 0.27 would be required. The thickness of a 54-cycle film is about 44 layers (i.e. two layers of Pd-porphyrin plus 42 layers of free-base porphyrin). The quantity (0.27/0.5) x 44 (= 24 layers) gives an estimate of the number of layers that are non-emissive and sited between the light source and the emissive layers (which number 20 layers (= 44 -24)). Of the 24 non-emissive layers, 22 contain free-base porphyrins. This quantity (22) can be equated with the average number of layers an exciton can traverse. If we instead assume that all 42 free-base porphyrin layers are equally illuminated, i.e. we neglect inner-filter effects, we conclude that the exciton traverses 26 layers (= 0.62 x 42 layers). Clearly, inner-filter effects need to be taken into account for films absorbing this strongly.
45. If we assume that 22 layers is a reasonable approximation for the root mean square displacement of the exciton characterized by a 9 ns lifetime, we find that the average number of chromophore-to-chromophore energy-transfer steps (exciton hopping steps) is ~484 (= 222) and time required for each hop is ~20 ps. Notably, this value is 3 to 4 times shorter than the lifetime of the quenching-resistant chromophore sub-population discussed above. In turn, these observations imply that the exciton associated with the short fluorescence time is less mobile (i.e. is characterized by a substantially longer chromophore-to-chromophore hopping rate) than the exciton associated with 9 ns fluorescence.
46. A reviewer has suggested that we consider, specifically for 4,4'-bipyridine, pillaring-ligand-mediated electronic communication between porphyrin layers (i.e., a through-bond pathway) as a mechanism for energy transfer. Contributions from a through-bond (super-exchange) pathway could be important for electron or hole transfer, but the rate of through-bond energy transfer (Dexter transfer) falls off much more rapidly with separation distance than does the rate of electron or hole transfer. Further, the bond-connectivity is not especially favorable for Dexter transfer: the pillars are geometrically orthogonal to the chromophore; the intervening Zn(II) nodes are closed-shell d10 ions, so are of little value in facilitating electronic coupling;

and the chromophore is further separated from the pillaring ligands by out-of-plane phenyl-carboxylate substituents. While important for certain other systems (see refference 3), we consider through-bond coupling to be of negligible importance for facilitating energy-transfer for the systems examined here
47. Maza, W. A.; Padilla, R.; Morris, A. J., Concentration Dependent Dimensionality of Resonance Energy Transfer in a Postsynthetically Doped Morphologically Homologous Analogue of UIO-67 MOF with a Ruthenium(II) Polypyridyl Complex. *J. Am. Chem. Soc.* **2015,** *137*, 8161-8168.
48. Kent, C. A.; Liu, D.; Meyer, T. J.; Lin, W., Amplified Luminescence Quenching of Phosphorescent Metal–Organic Frameworks. *J. Am. Chem. Soc.* **2012,** *134*, 3991-3994.
49. Kent, C. A.; Mehl, B. P.; Ma, L.; Papanikolas, J. M.; Meyer, T. J.; Lin, W., Energy Transfer Dynamics in Metal−Organic Frameworks. *J. Am. Chem. Soc.* **2010,** *132*, 12767-12769.
50. Palomaki, P. K. B.; Civic, M. R.; Dinolfo, P. H., Photocurrent Enhancement by Multilayered Porphyrin Sensitizers in a Photoelectrochemical Cell. *ACS Appl. Mater. Interfaces* **2013,** *5*, 7604-7612.
51. Huijser, A.; Suijkerbuijk, B. M. J. M.; Klein Gebbink, R. J. M.; Savenije, T. J.; Siebbeles, Efficient Exciton Transport in Layers of Self-Assembled Porphyrin Derivatives. *J. Am. Chem. Soc.* **2008,** *130*, 2485-2492.
52. Gouterman, M., Spectra of Porphyrins. *J. Mol. Spectrosc.* **1961,** *6*, 138-163.
53. Richert, S.; Bullard, G.; Rawson, J.; Angiolillo, P. J.; Therien, M. J.; Timmel, C. R., On the Importance of Electronic Symmetry for Triplet State Delocalization. *J. Am. Chem. Soc.* **2017,** *139*, 5301-5304.
54. Mandal, A. K.; Taniguchi, M.; Diers, J. R.; Niedzwiedzki, D. M.; Kirmaier, C.; Lindsey, J. S.; Bocian, D. F.; Holten, D., Photophysical Properties and Electronic Structure of Porphyrins Bearing Zero to Four Meso-Phenyl Substituents: New Insights into Seemingly Well Understood Tetrapyrroles. *J. Phys. Chem. A* **2016,** *120*, 9719-9731.
55. Masi Reddy, N.; Pan, T.-Y.; Christu Rajan, Y.; Guo, B.-C.; Lan, C.-M.; Wei-Guang Diau, E.; Yeh, C.-Y., Porphyrin Sensitizers with [π]-Extended Pull Units for Dye-Sensitized Solar Cells. *PCCP* **2013,** *15*, 8409-8415.
56. Chang, Y.-C.; Wang, C.-L.; Pan, T.-Y.; Hong, S.-H.; Lan, C.-M.; Kuo, H.-H.; Lo, C.-F.; Hsu, H.-Y.; Lin, C.-Y.; Diau, E. W.-G., A Strategy to Design Highly Efficient Porphyrin Sensitizers for Dye-Sensitized Solar Cells. *Chem. Commun.* **2011,** *47*, 8910-8912.

TOC Graphic:

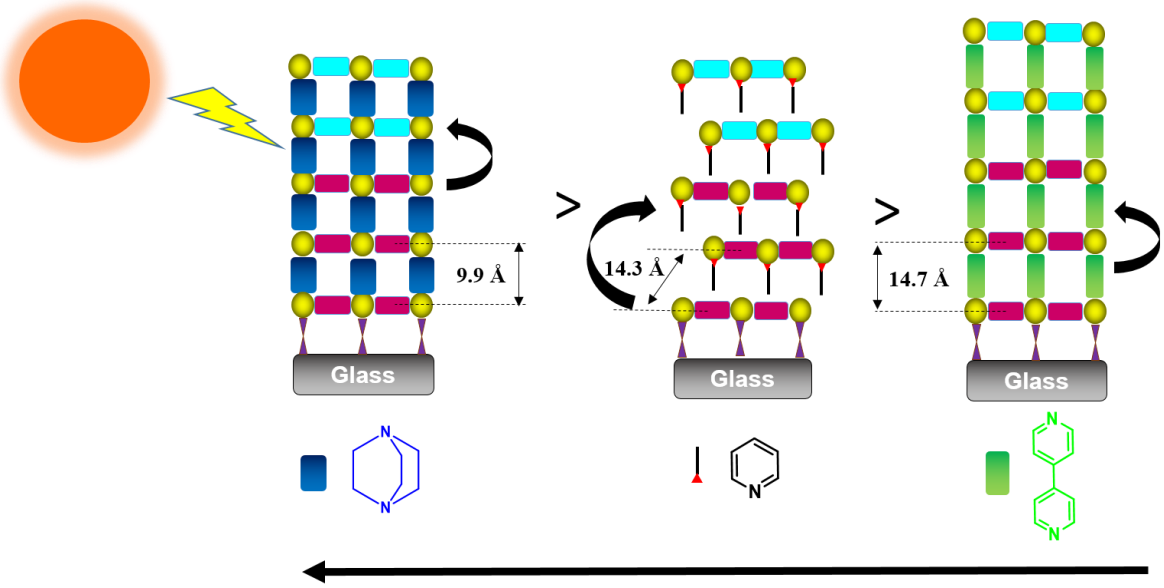

Increase in number of chromophoric layers exciton traverses